JOURNAL OF SPACECRAFT AND ROCKETS
Vol. 42, No. 5, September–October 2005

# Orbit Determination Strategy Using Single-Frequency Global-Positioning-System Data

Yoola Hwang*
*Electronics and Telecommunications Research Institute, Daejeon 305-350, Republic of Korea*
and
George H. Born†
*University of Colorado, Boulder, Colorado 80309*

**Orbit determination results are presented for a low-Earth-orbiter (LEO) satellite carrying a single-frequency global-positioning-system (GPS) receiver. Various techniques to correct for errors induced by ionospheric refraction are compared. These include the Jet Propulsion Laboratory's (JPL) global ionosphere maps (GIM), which provide global maps of total electron content. The direct-calibration method, differenced range versus integrated Doppler (DRVID), which uses range differences of group delay and phase advance to compensate for the first-order ionospheric error, was also tested. The fidelity of the orbit solutions was compared using orbit overlaps and orbit differences from dual-frequency truth orbits computed using MicroCosm and JPL's Gipsy-Oasis-II program. Analyses showed that, with a single-frequency GPS receiver on the LEO satellite, the DRVID-corrected carrier phase can determine the orbit with accuracy below the meter level. JPL's GIM correction to pseudorange data also provided improved results over no ionospheric error correction.**

## Nomenclature

| | | |
|---|---|---|
| $c$ | = | speed of light, m/s |
| $E_{\mathrm{LEO}}$ | = | elevation angle of global-positioning-system (GPS) satellites at the low-Earth-orbit (LEO) satellite position |
| $H$ | = | scale height (=100 km), m |
| $h_{\mathrm{IPP}}$ | = | height from ground to the ionospheric pierce point (IPP), m |
| $h_{\mathrm{LEO}}$ | = | altitude of the LEO satellite, m |
| $h_0$ | = | peak point of the ionospheric density, m |
| $N$ | = | integer ambiguity |
| $P1$, $P2$ | = | pseudorange observable on GPS L1 and L2 frequency, respectively |
| $r_{\mathrm{IPP}}$ | = | distance from the Earth center to the IPP, m |
| $r_{\mathrm{LEO}}$ | = | LEO satellite radial position magnitude, m |
| $sf(E_{\mathrm{LEO}})$ | = | slant function |
| $t_k$, $t_0$ | = | tagging time of measurement for arbitrary epoch $k$ and minimum range epoch 0 during the phase lock, respectively, s |
| $\alpha$ | = | scale factor |
| $\Delta\rho_{\mathrm{ion}}$ | = | ionospheric range delay, m |
| $\lambda_{\mathrm{IPP}}$, $\varphi_{\mathrm{IPP}}$ | = | longitude and latitude of the IPP, respectively |
| $\rho_R^S$ | = | geometric range from the GPS satellite transmitter to the LEO receiver antenna, m |
| $\Phi_1$ | = | carrier phase range observable on GPS L1 frequency |

## Introduction

THE global positioning system (GPS) has played an important role in generating precise orbit solutions because it provides global and continuous high-precision observation data. However, the transmitted GPS signal contains measurement errors such as ionospheric delay, multipath, and instrumental noise. The magnitude of ionospheric delay in GPS measurements ranges from a few centimeters to tens of meters, and the positioning error caused by the ionosphere can reach as high as 150 m during high solar activity such as during the year 2002. Hence, the ionospheric error should be corrected to enhance the accuracy of the orbit solutions.

To reduce the ionospheric error, a method based on ionosphere models or the use of group and phase ionospheric calibration (GRAPHIC) technique that averages carrier phase and pseudorange has been tried for single-frequency GPS users.[1–5] Using this technique, precise orbit determination for the mission of TOPEX/POSEIDON (T/P) showed orbit accuracy at a few centimeter level in the radial direction with single-frequency GPS data.[2,6,7] However, at 1334 km the T/P spacecraft is above much of the ionosphere. The orbit solution of the Extreme Ultra Violet Explorer (500-km altitude) was obtained at the level of 1 m rss in a three-dimensional (1-$\sigma$) sense for a single-frequency ionosphere calibration with the techniques of reduced dynamic model and empirical acceleration estimates.[8] Montenbruck and Gill[3] and Yoon et al.[4] improved point positioning accuracy for a low-Earth-orbiter (LEO) satellite through the use of the International Reference Ionosphere model, which was modified by estimating a scale factor with the position and velocity of the satellite. In Montenbruck's[5] recent research on the ionospheric error correction for a LEO satellite, he showed orbit accuracy at the 1–1.5-m rms level for a purely kinematic GPS solution using the GRAPHIC technique to correct ionospheric errors. The GRAPHIC technique is very similar to the differenced range vs integrated-Doppler (DRVID) technique used here.

The challenging minisatellite payload (CHAMP) orbit, at an altitude of 454 km, is near circular and near polar ($i = 87$ deg) to allow a homogeneous and global coverage of the Earth. Because the CHAMP satellite is at a low altitude and carries a "BlackJack" GPS receiver, which is codeless and dual frequency, it is useful for evaluating the effects of ionospheric error on orbit determination accuracy. CHAMP orbits based on dual-frequency data have overlaps statistics consistent with orbit accuracy on the order of 10 cm in a three-dimensional (1-$\sigma$) sense.[9,10]

Here we focus on using the CHAMP satellite to demonstrate the accuracy that could be obtained with single- and dual-frequency solutions. In particular, two approaches are investigated to correct the ionospheric induced measurement error: the ionospheric shell model of Jet Propulsion Laboratory's (JPL) global ionosphere

Presented as AAS Paper 2004-222 at the AAS/AIAA Space Flight Mechanics Conference, Maui, HI, 8–12 February 2004; received 28 March 2004; revision received 17 August 2004; accepted for publication 30 August 2004. 

*Senior Research Staff, Communication Satellite Research Group. Member AIAA.
†Professor and Director, Colorado Center for Astrodynamics Research. Fellow AIAA.

maps[11] (GIM) and DRVID,[12] applied to double-differenced range and phase measurements. The GIM product provides the total electron content (TEC) between the ground and the GPS constellation altitude. We then use a predicted scale factor for the ionospheric range to account for the TEC between the LEO and GPS altitudes. A modified DRVID method assuming zero bias at the minimum range epoch over a pass and estimating a pass-by-pass range bias provides more precise orbit solution than the GIM approach.

## JPL's GIM with Scale Factor

Dual-frequency users can eliminate the ionospheric error by combining measurements that have two different frequencies ($f_1 = 1575.42$, $f_2 = 1227.6$ MHz). However, single-frequency users must either use ionospheric models or use a combined phase and pseudorange data set to correct the ionospheric error unless they simply choose to neglect this error.

JPL generates the GIM of vertical TEC from approximately 100 GPS sites.[11] The vertical TEC was interpolated by using a quadratic weighting function to yield the TEC at the ionospheric pierce point, which is the intersection point between the mean height of ionosphere and the line of sight of the LEO satellite. The JPL's GIM products can supply ionospheric range delay at the altitude of the LEO satellite by applying a scale factor to the TEC in the path from the ground. Montenbruck and Gill[3] introduced the scale factor used here for the ionospheric delay at the LEO satellite altitude. The scale factor is given by

$$\alpha = \frac{\mathrm{TEC}(\lambda_{\mathrm{IPP}}, \varphi_{\mathrm{IPP}}, h_{\mathrm{IPP}})}{\mathrm{TEC}(\lambda_{\mathrm{IPP}}, \varphi_{\mathrm{IPP}}, 0)} = \frac{\frac{1}{2}\left(e - \exp\{1 - \exp[-(h_{\mathrm{LEO}} - h_0)/H]\}\right)}{e - \exp[1 - \exp(h_0/H)]} \tag{1}$$

The predicted scale factor that relates the $\mathrm{TEC}(\lambda_{\mathrm{IPP}}, \varphi_{\mathrm{IPP}}, h_{\mathrm{IPP}})$ of the ionosphere above $h_{\mathrm{IPP}}$ to the $\mathrm{TEC}(\lambda_{\mathrm{IPP}}, \varphi_{\mathrm{IPP}}, 0)$ above ground was calculated at each epoch according to the altitude $h_{\mathrm{LEO}}$. As shown in Eq. (2), the ionospheric range error at each measurement epoch is calculated with a scale factor given by Eq. (1).

$$\Delta\rho_{\mathrm{ion}}(t_k) = \alpha\left(40.3 \Big/ f_1^2\right)\mathrm{TEC}(\lambda_{\mathrm{IPP}}, \varphi_{\mathrm{IPP}}, 0) sf(E_{\mathrm{LEO}}) \tag{2}$$

The slant function, which accounts for the increase in path length with decreasing elevation caused by the ionosphere, is given by[3]

$$sf(E_{\mathrm{LEO}}) = 1 \Big/ \sqrt{1 - [\cos(E_{\mathrm{LEO}})/(r_{\mathrm{IPP}}/r_{\mathrm{LEO}})]^2} \tag{3}$$

This slant function becomes less accurate at low elevation angles, and as a result data below 10-deg elevation are edited for the orbit-determination (OD) solution.

## Differenced Range vs Integrated Doppler

The DRVID technique uses the property that the group delay and phase advance have the same magnitude but opposite sign. The combination of range-differenced pseudorange group delay and phase advance removes the first-order ionospheric delay of the measurement. Here the DRVID technique calculates range differenced ionospheric error between coarse-acquisition (C/A) code pseudorange and carrier phase on the L1 frequency. To calculate the range-differenced ionospheric error, we subtract the observations at two different epochs as long as the receiver has kept a continuous lock on the carrier signal. The range and phase changes over interval are given by

$$P1(t_k) - P1(t_0) = \rho_R^S(t_k) - \rho_R^S(t_0) + \left(40.3 \Big/ f_1^2\right)[\mathrm{TEC}(t_k) - \mathrm{TEC}(t_0)] \tag{4}$$

$$\Phi_1(t_k) - \Phi_1(t_0) = \rho_R^S(t_k) - \rho_R^S(t_0) - \left(40.3 \Big/ f_1^2\right) \times [\mathrm{TEC}(t_k) - \mathrm{TEC}(t_0)] + [N(t_k) - N(t_0)](c/f_1) \tag{5}$$

Both equations ignore all other measurement errors except ionospheric delay. Equations (4) and (5) are combined to obtain the ionospheric error $\Delta\rho_{\mathrm{ion}}(t_k)$ at an arbitrary epoch by DRVID as shown in Eq. (6). The integer terms in Eq. (5) canceled out each other because they have same number over a pass:

$$\Delta\rho_{\mathrm{ion}}(t_k) = \left(40.3 \Big/ f_1^2\right)[\mathrm{TEC}(t_k) - \mathrm{TEC}(t_0)] = \{[P1(t_k) - P1(t_0)] - [\Phi_1(t_k) - \Phi_1(t_0)]\}/2 + \Delta\rho_{\mathrm{ion}}(t_0) \tag{6}$$

$$\Delta\rho_{\mathrm{ion}}(t_0) = \left(40.3 \Big/ f_1^2\right)\mathrm{TEC}(t_0) \approx 0 \tag{7}$$

The ionospheric induced measurement error can be corrected by adding the calculated ionospheric error of Eq. (6) to each pseudorange and carrier phase observable. Here, the range-differenced DRVID assume zero bias at the minimum range epoch (i.e., the greatest elevation angle) over a pass to eliminate the calculation of the unknown constant range correction as indicated in Eq. (7). Any remaining bias was removed by estimating a pass-by-pass range bias during the orbit determination.

## Ionospheric Error with Differential Code Bias

The accuracy of the ionospheric error correction by either JPL's GIM product with a scale factor or the DRVID method can be evaluated by comparing the ionospheric delay computed from the combination of the dual-frequency GPS data. Equation (8) yields the ionospheric delay calculated by dual frequency at the L1 frequency:

$$\Delta\rho_{\mathrm{ion}}(t_k) = \frac{[P2(t_k) - P1(t_k)]}{\left[(f_1/f_2)^2 - 1\right]} \tag{8}$$

Note that the differential code bias (DCB) of the dual-frequency BlackJack receiver was known to be about 2.4 m (8 ns) between the L1 and L2 code phase measurements.[3] This was calibrated before the CHAMP satellite was launched.

Figure 1 shows the ionospheric error at the L1 GPS frequency from the dual-frequency BlackJack pseudorange data and JPL's GIM product after applying a scale factor for GPS PRN 7 on 22 May 2001 (elevation cutoff of 0 deg for Figs. 1–4). The ionospheric error value from JPL's GIM products was adjusted by a linear fit to the dual-frequency ionospheric delay value as seen in Fig. 2. Here, JPL's GIM results show a 2.8-m offset from the dual-frequency ionospheric delay, which is close to the DCB of the CHAMP receiver. Figure 3 displays the dual-frequency ionospheric delay with DRVID results for GPS PRN 7 on 22 May 2001. The bias between the dual-frequency ionospheric delay and that computed by JPL's GIM is smaller than that computed from DRVID as shown in Fig. 4. The DRVID has a larger bias than BlackJack's DCB because of the zero-bias assumption at the minimum range epoch as well as additional systematic biases.

## Dynamic Model Approach

A dynamic model approach based on global and continuous GPS tracking data was used for the OD in this research. A 30-h arc length was selected for the orbit estimate. The OD for the LEO satellite was computed using MicroCosm.[13] MicroCosm uses a high-fidelity dynamic model consisting of the following: 1) EGM-96 gravity model complete to degree and order 70; 2) Jacchia-71 atmospheric density model; 3) tabular data consisting of solar flux, geomagnetic data, and Earth orientation parameters (updated on a weekly basis); and 4) planetary ephemerides to account for $n$-body perturbations.[14] In addition, the position, velocity, one drag coefficient per arc, one solar pressure coefficient per arc, and 1.5-h empirical acceleration coefficients for the along-track and cross-track components were estimated to compensate for mismodeled or unmodeled dynamic error. The tropospheric delay is also estimated once per arc.

The GPS measurement is restricted to C/A code and L1 carrier phase when considering single-frequency data only.[14,15] To remove clock errors, we use double-differenced GPS measurements, which

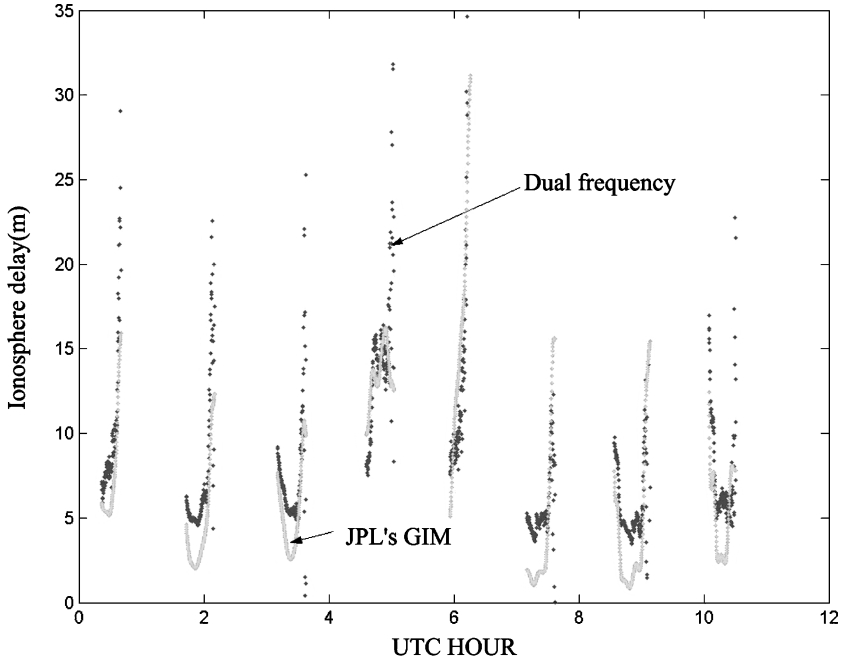


**Fig. 1 Dual-frequency ionospheric delay and JPL's GIM products with scale factor for GPS PRN 7 (22 May 2001).**

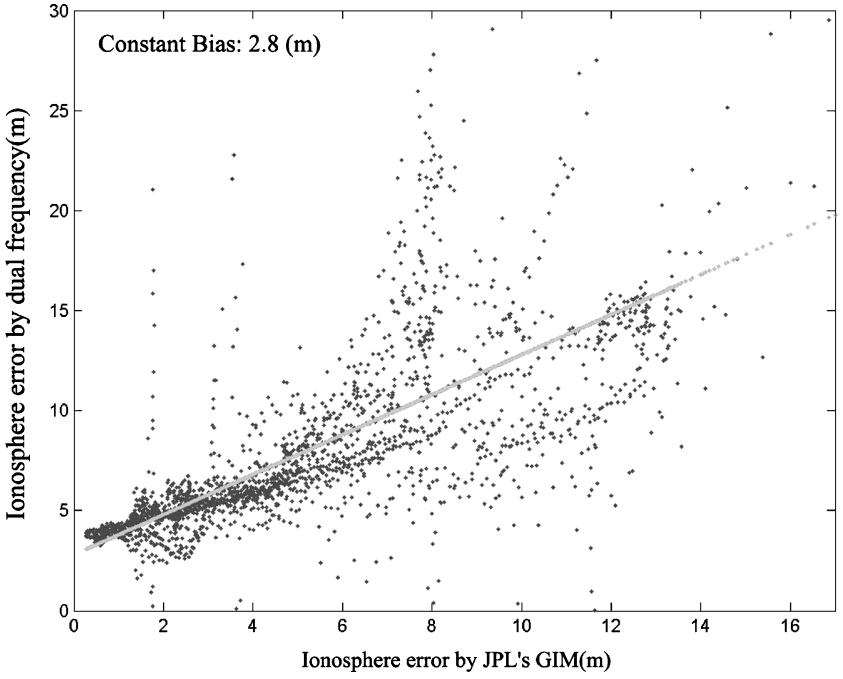


**Fig. 2 Linear fit of ionosphere error using JPL's GIM to dual-frequency ionospheric delay.**

are derived from two GPS satellites, the LEO satellite, and one ground station. The dual-frequency GPS data are used to eliminate the ionospheric error between GPS satellite and ground station. The calculated ionospheric errors are used to correct the GPS pseudorange and carrier phase observable of the LEO satellite directly during data processing.

## Measurement RMS

The rms value of double-differenced tracking residuals is one indicator of orbit accuracy. However, small rms values are a necessary but not sufficient condition for absolute orbit accuracy. Table 1 shows the rms of tracking data residuals for all cases using carrier phase and pseudorange from the various ionospheric error correction techniques employed in this research. The estimate of a measurement bias for each pass of data helped to reduce the postfit residual values in the DRVID pseudorange case because the ionospheric bias of each pseudorange pass as well as systematic biases are absorbed by the estimated measurement bias. As expected, the dual-frequency method using carrier phase data showed the smallest rms of residuals. The model-based JPL's GIM method also has an improved rms value when compared with the rms value with no ionospheric error correction. Here the case with no ionospheric error correction applied is based on L1 pseudorange data.

## Orbit Overlaps

The dynamic orbit solutions obtained using MicroCosm are based on a 30-h arc length, including six hours of common data with the adjacent arc. The 10-day data set for the CHAMP satellite over 20–29 January 2002 was broken into 10 30-h arcs. The central four hours of the six-hour common data arcs are used to compute orbit

**Table 1 RMS of postfit residual for CHAMP data[a]**

| Date[b] | Dual-frequency carrier phase | Dual-frequency pseudorange | DRVID carrier phase | DRVID pseudorange | JPL's GIM pseudorange | Uncorrected pseudorange |
|---|---|---|---|---|---|---|
| 20 Jan. | 0.049 | 1.57 | 0.12 | 1.01 | 2.53 | 4.38 |
| 21 Jan. | 0.045 | 1.55 | 0.11 | 0.99 | 2.37 | 3.78 |
| 22 Jan. | 0.045 | 1.56 | 0.11 | 0.98 | 2.50 | 4.00 |
| 23 Jan. | 0.046 | 1.56 | 0.11 | 0.93 | 2.40 | 4.22 |
| 24 Jan. | 0.043 | 1.56 | 0.11 | 1.01 | 2.46 | 4.06 |
| 25 Jan. | 0.051 | 1.57 | 0.11 | 0.96 | 2.41 | 4.24 |
| 26 Jan. | 0.045 | 1.53 | 0.11 | 0.94 | 2.44 | 4.59 |
| 27 Jan. | 0.054 | 1.57 | 0.11 | 0.96 | 2.41 | 4.52 |
| 28 Jan. | 0.050 | 1.53 | 0.11 | 0.92 | 2.49 | 4.79 |
| 29 Jan. | 0.048 | 1.64 | 0.11 | 0.89 | 2.42 | 4.89 |

[a]Units are meters. [b]2002.

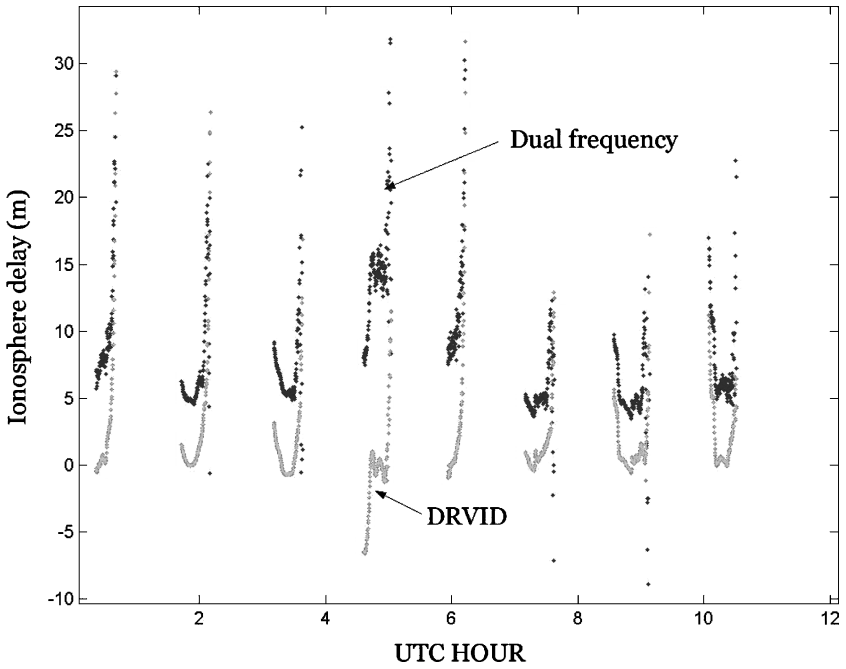


**Fig. 3 Dual-frequency ionospheric delay and DRVID with zero-bias assumption for GPS PRN 7 (22 May 2001).**

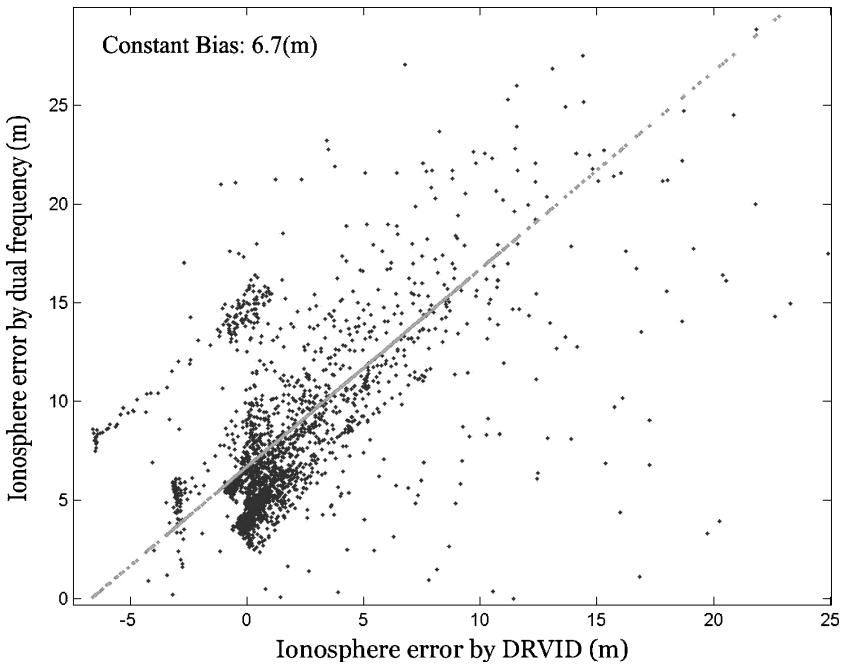


**Fig. 4 Linear fit of ionosphere error using DRVID method to dual-frequency ionospheric delay.**

**Table 2 Four-hour orbit overlap rms and three-dimensional rss values[a]**

| Date | R | T | N | 3D[b] | R | T | N | 3D | R | T | N | 3D |
|---|---|---|---|---|---|---|---|---|---|---|---|---|
| | *Dual-frequency carrier phase* | | | | *Dual-frequency pseudorange* | | | | *DRVID carrier phase* | | | |
| 20–21 Jan. | 2.8 | 5.6 | 3.2 | 7.0 | 5.5 | 10.3 | 5.9 | 13.1 | 7.5 | 13.5 | 6.7 | 16.8 |
| 21–22 Jan. | 2.9 | 6.2 | 5.5 | 8.8 | 6.2 | 11.5 | 11.8 | 17.6 | 5.5 | 11.7 | 12.7 | 18.1 |
| 22–23 Jan. | 1.9 | 4.3 | 2.5 | 5.3 | 3.9 | 7.3 | 6.5 | 10.5 | 4.3 | 9.9 | 5.6 | 12.2 |
| 23–24 Jan. | 6.3 | 12.2 | 4.4 | 14.4 | 6.6 | 16.4 | 14.4 | 22.8 | 3.6 | 8.4 | 5.1 | 10.5 |
| 24–25 Jan. | 2.4 | 4.3 | 4.6 | 6.7 | 14.6 | 33.5 | 10.3 | 38.0 | 2.6 | 8.0 | 7.7 | 11.4 |
| 25–26 Jan. | 6.9 | 10.1 | 8.3 | 14.8 | 9.5 | 18.8 | 5.9 | 21.9 | 7.8 | 12.6 | 8.5 | 17.1 |
| 26–27 Jan. | 2.7 | 6.0 | 10.1 | 12.1 | 12.1 | 21.6 | 8.8 | 26.3 | 6.3 | 11.5 | 8.3 | 15.5 |
| 27–28 Jan. | 7.1 | 16.7 | 11.4 | 21.4 | 4.0 | 7.2 | 4.6 | 9.4 | 5.3 | 9.7 | 10.5 | 15.2 |
| 28–29 Jan. | 4.9 | 10.6 | 11.0 | 16.0 | 28.0 | 53.8 | 22.4 | 64.7 | 7.3 | 18.3 | 11.5 | 22.8 |
| | *DRVID pseudorange* | | | | *JPL's GIM pseudorange* | | | | *Uncorrected pseudorange* | | | |
| 20–21 Jan. | 18.6 | 40.1 | 28.8 | 52.8 | 19.7 | 42.2 | 25.0 | 52.9 | 20.8 | 45.5 | 33.5 | 60.2 |
| 21–22 Jan. | 4.8 | 13.2 | 5.3 | 15.0 | 32.9 | 64.6 | 53.8 | 90.3 | 42.4 | 90.1 | 65.8 | 119.4 |
| 22–23 Jan. | 12.0 | 24.7 | 26.1 | 37.9 | 15.4 | 38.1 | 17.2 | 44.5 | 18.1 | 39.0 | 20.1 | 47.5 |
| 23–24 Jan. | 6.4 | 18.6 | 11.6 | 22.8 | 26.9 | 49.3 | 18.8 | 59.2 | 29.1 | 56.1 | 49.0 | 80.0 |
| 24–25 Jan. | 13.9 | 38.7 | 34.0 | 53.4 | 26.2 | 46.4 | 33.5 | 62.9 | 33.0 | 61.4 | 69.7 | 98.6 |
| 25–26 Jan. | 17.7 | 31.8 | 11.8 | 38.3 | 22.4 | 44.1 | 21.5 | 53.9 | 29.0 | 61.2 | 30.8 | 74.4 |
| 26–27 Jan. | 13.0 | 27.2 | 23.4 | 38.2 | 15.5 | 29.8 | 12.3 | 35.8 | 88.3 | 174.9 | 20.3 | 197.0 |
| 27–28 Jan. | 12.0 | 31.0 | 8.1 | 34.2 | 28.0 | 51.5 | 22.2 | 62.7 | 78.3 | 156.2 | 35.7 | 178.3 |
| 28–29 Jan. | 10.4 | 23.0 | 9.7 | 27.0 | 14.3 | 28.9 | 10.9 | 34.0 | 51.0 | 103.8 | 26.0 | 118.5 |

[a]Units are centimeters. [b]Three dimensional.

**Table 3 RMS orbit differences over 10 days for solutions using MicroCosm[a]**

| 20–29 Jan.[b] | Dual-frequency pseudorange | DRVID carrier phase | DRVID pseudorange | JPL's GIM pseudorange | Uncorrected pseudorange |
|---|---|---|---|---|---|
| R | 0.216 | 0.109 | 0.377 | 0.571 | 0.868 |
| T | 0.504 | 0.318 | 1.000 | 1.339 | 2.402 |
| N | 0.323 | 0.129 | 0.415 | 0.792 | 1.288 |
| rss | 0.637 | 0.360 | 1.146 | 1.658 | 2.861 |

[a]Units are meters. [b]2002.

overlap statistics. In the orbit overlap evaluation, the orbit difference levels showed several tens of centimeters in a three-dimensional rss sense for the various correction methods (Table 2). In general, the statistics of the overlapping orbit solution are a good indicator of orbit precision, but are only a relative measure.[2] The overlap statistics can tend to overestimate the true orbit error caused by the amplification of errors at either end of the overlap period. Therefore, four-hour orbit overlap data in the middle of the six-hour overlap period were used to avoid these end effects.

## Comparison-with-Truth Orbit

The comparison-with-truth orbits is a direct method to evaluate the accuracy of orbit solutions generated by MicroCosm. Here the truth orbit is defined as the orbit solution determined by MicroCosm using dual-frequency double-differenced carrier phase data from CHAMP. The differences of the orbits for a 24-h period, which is extracted from a 27-h or 30-h orbit arc, were calculated during a period 20–29 January 2002. We used a data set from 2002 to observe the orbit solutions during a period of high solar activity. Table 3 presents the differences between the truth orbits and various ionosphere corrected orbits. For example, the orbit difference over 10 days showed a three-dimensional rss of about 36 cm between MicroCosm orbits based on dual-frequency carrier phase measurements and those using DRVID carrier phase.

## Comparison of MicroCosm and Gipsy-Oasis-II Solutions

As another validation of the orbit solutions, orbits generated by other institutions were used. In this section the truth orbit is defined as the orbit solution generated by the Gipsy-Oasis-II (GOA II) program from the JPL. The 24-h orbit in the middle of a 30-h arc determined by MicroCosm was compared with JPL's Precision Orbit Ephemeris (POE)[‡] for 20–29 January 2002. JPL's measurement data used are dual-frequency pseudorange and carrier phase. The data interval is 30 s, and the arc length is 27 h. The orbit solution, based on the dynamic and reduced dynamic technique, is performed, and unmodeled accelerations are estimated as stochastic parameters. The GPS orbits and clocks are fixed at the values determined by JPL's quick-look products. Six initial conditions for the CHAMP satellite's position and velocity are estimated along with a drag coefficient, a solar radiation pressure coefficient, and stochastic accelerations in the radial, along-track, and cross-track directions.

Both MicroCosm and GOA II can produce orbits internally in the inertial J2000 reference frame. The orbits were compared in the inertial J2000 reference frame. The orbit determined by the DRVID carrier phase has a 55-cm three-dimensional rss difference from JPL's POE over 10 days (Table 4). The ionospheric bias of DRVID carrier phase is absorbed in the integer ambiguity during the double-differenced measurement bias estimate. In Table 4, the DRVID pseudorange result shows differences with JPL's POE of 1.23-m three-dimensional rss, whereas DRVID carrier phase results in 0.55-m rss. The DRVID carrier phase is more accurate than DRVID pseudorange because the measurement has less noise than the pseudorange. Here the three-dimensional rss orbit difference between JPL's POE and the orbit estimated using JPL's GIM products with a scale factor is 1.67 m, indicating that the GIM correction is not as accurate as the DRVID. The GIM results could be improved with more ground stations contributing to the maps. In fact JPL is now using about 700 stations to generate the GIM product instead of the 100 used here. Even so, there are still large areas of the southern oceans where there is little or no coverage. The GIM results are

[‡]Data available online at ftp://sayatnova.jpl.nasa.gov/pub/genesis/orbits/champ/quick [cited 28 Oct. 2003].

**Table 4 RMS orbit differences over 10 days for JPL's POE and orbit using MicroCosm[a]**

| 20–29 Jan.[b] | Dual-frequency carrier phase | Dual-frequency pseudorange | DRVID carrier phase | DRVID pseudorange | JPL's GIM pseudorange | Uncorrected pseudorange |
|---|---|---|---|---|---|---|
| R | 0.154 | 0.181 | 0.173 | 0.397 | 0.577 | 0.874 |
| T | 0.314 | 0.387 | 0.435 | 1.062 | 1.340 | 2.380 |
| N | 0.277 | 0.347 | 0.292 | 0.486 | 0.820 | 1.321 |
| rss | 0.446 | 0.550 | 0.552 | 1.233 | 1.674 | 2.858 |

[a]Units are meters. [b]2002.

further degraded relative to DRVID by the use of an approximating scale factor to obtain the TEC between CHAMP spacecraft and the GPS constellation. Estimating a pass-by-pass range bias did not improve the GIM results.

Different arc length of the orbits as well as different dynamic model and filter contribute to the differences in the orbits determined by MicroCosm and JPL's POE.

## Conclusions

In this paper, the correction of ionospheric error has been analyzed assuming a low-Earth-orbit satellite equipped with a single-frequency global-positioning-system receiver. The orbit determination based on the dynamic model approach included ionospheric correction by either Jet Propulsion Laboratory's global ionospheric maps (GIM) products with a scale factor or the differenced range versus integrated Doppler (DRVID) method. Both methods showed significantly improved orbit accuracy over not correcting for ionospheric error when compared to the truth orbits based on dual-frequency data.

Through this research, DRVID carrier phase was determined to be the best way to reduce ionospheric error for single-frequency users. The DRVID-corrected carrier phase with pass-by-pass range bias estimates resulted in three-dimensional rss orbit errors on the order of 55 cm. This is more than an 80% reduction over no ionospheric correction. If carrier phase is not available, the model-based method using the GIM product with a scale factor also provided significant improvement over no ionospheric error correction.

## References

[1]Bertiger, W. I., and Wu, S. C., "Single Frequency GPS Orbit Determination for Low Earth Orbiters," *Proceedings of 96 ION GPS Conference National Technical Meeting*, Inst. of Navigation, Alexandria, VA, 1996, pp. 463–473.

[2]Haines, B. J., Lichten, S. M., Lough, M. F., Muellerschoen, R. J., and Vigue-Rodi, Y., "Determining Precise Orbits for TOPEX/POSEIDON Within One Day of Real Time: Results and Implications," *Advances in the Astronautical Sciences*, Vol. 102, Pt. 1, 1999, pp. 623–634.

[3]Montenbruck, O., and Gill, E., "Ionospheric Correction for GPS Tracking of LEO Satellites," *Journal of Navigation*, Vol. 55, No. 2, 2002, pp. 293–304.

[4]Yoon, J. C., Roh, K. M., Park, E. S., Moon, B. Y., Choi, K. H., Lee, J. S., Lee, B. S., Kim, J., and Chang, Y. K., "Orbit Determination of Spacecraft Using Global Positioning System Single-Frequency Measurement," *Journal of Spacecraft and Rockets*, Vol. 39, No. 5, 2002, pp. 796–801.

[5]Montenbruck, O., "Kinematic GPS Positioning of LEO Satellites Using Ionosphere-Free Single Frequency Measurements," *Aerospace Science and Technology*, Vol. 7, No. 5, 2003, pp. 331–405.

[6]Muellerschoen, R. J., Bertiger, W. I., Wu, S. C., Munson, T. N., Zumberge, J. F., and Haines, B., "Accuracy of GPS Determined TOPEX/POSEIDON Orbits During Anti-Spoof Periods," *Proceedings of 94 ION GPS Conference National Technical Meeting*, Inst. of Navigation, Alexandria, VA, 1994, pp. 607–614.

[7]Nouël, F., Berthias, J. P., Delouze, M., Guitart, A., Laudet, P., Piuzzi, A., Pralines, D., Valorge, C., Dejoie, C., Susini, M. F., and Taburiau, D., "Precise Centre National d'Etudes Spatiales Orbits for TOPEX/POSEIDON: Is Reaching 2 cm Still a Challenge?," *Journal of Geophysics Research*, Vol. 99, No. C12, 1994, pp. 24,405–24,419.

[8]Gold, K., "GPS Obit Determination for the EXTREME ULTRA VIOLET EXPLORER," Ph.D. Dissertation, Aerospace Engineering Sciences, Univ. of Colorado, Boulder, CO, Nov. 1994.

[9]Kuang, D., Bar-Sever, Y., Bertiger, W., Desai, S., Haines, B., Iijima, B., Kruizinga, G., Meehan, T., and Romans, L., "Precise Orbit Determination for CHAMP Using GPS Data from BlackJack Receiver," *Proceedings of 01 ION GPS Conference National Technical Meeting*, Inst. of Navigation, Alexandria, VA, 2001, pp. 762–770.

[10]Rim, H., Kang, Z., Nagel, P., Yoon, S., Bettadpur, S., Schutz, B., and Tapley, B., "CHAMP Precision Orbit Determination," *Advances in the Astronautical Sciences*, Vol. 109, Pt. 1, 2001, pp. 403–500.

[11]Mannucci, A. J., Wilson, B. D., Yuan, D. N., Ho, C. H., Lindqwister, U. J., and Runge, T. F., "A Global Mapping Technique for GPS-Derived Ionospheric Total Electron Content Measurements," *Radio Science*, Vol. 33, No. 3, 1998, pp. 565–582.

[12]MacDoran, P. F., and Martin, W. L., "A First Principles Derivation of Differenced Range Versus Integrated Doppler (DRVID) Charged Particle Calibration Method," *JPL Space Program Summary*, Vol. 2, No. 3, 1970, pp. 37–62.

[13]Martin, T., *MicroCosm® Software Manuals*, ver. 1999, Van Martin Systems, Inc., Rockville, MD, Nov. 2000, Chap. 3.

[14]Meek, M., Gold, K., Hwang, Y., Axelrad, P., and Born, G., "Orbit Determination for the Quickbird Spacecraft," Core Technologies for Space Systems Conf., Nov. 2002.

[15]Lee, B. S., Lee, J. S., Kim, J. H., Lee, S. P., Kim, H. D., Kim, E. K., and Choi, H. J., "Operational Report of the Mission Analysis and Planning System for the KOMPSAT-I," *ETRI Journal*, Vol. 25, No. 5, 2003, pp. 387–400.

D. Spencer
*Associate Editor*